Experimental investigation of the effects of air pocket configuration on fluid transients in a pipeline

Jane Alexander[1], Zhao Li[2], Pedro J. Lee[3], Mark Davidson[4], and Huan-Feng Duan[5]

[1]Ph.D. Student, Department of Civil and Natural Resources Engineering, College of Engineering, University of Canterbury, Private Bag 4800, Christchurch 8020, New Zealand. Email: jane.alexander@pg.canterbury.ac.nz

[2]Senior Research Associate, Department of Civil and Natural Resources Engineering, College of Engineering, University of Canterbury, Christchurch 8020, New Zealand.

[3]Professor, Department of Civil and Natural Resources Engineering, College of Engineering, University of Canterbury, Christchurch 8020, New Zealand.

[4]Professor, Department of Civil and Natural Resources Engineering, College of Engineering, University of Canterbury, Christchurch 8020, New Zealand.

[5]Associate Professor, Department of Civil and Environmental Engineering, The Hong Kong Polytechnic University, Hung Hom, Kowloon, Hong Kong.

ABSTRACT

Air pockets entrapped in pipeline systems are required to be non-intrusively diagnosed by fluid transients. In this study, experimental investigations are used to compare the transient transmission and reflection effects of stationary in-line and off-line air pocket volumes along a pipe under zero base flow conditions. Comparison with theoretical modelling indicated that the difference in the transient response between the two configurations is primarily due to the inertia in the connecting water column associated with off-line air pockets. This means that the transient response depends on both the volume of the pocket and the dimensions of the cavity. Analysis in the frequency domain showed that the off-line air pocket may be characterised by the resonant frequency, at

which reflection is maximized, while the in-line pocket is characterized by a cut-off frequency above which there is little reflection. The damping of the transient signal may also be used to diagnose air, as the presence of air increases the damping rate by a factor of 3 to 4.

INTRODUCTION

A reliable water supply is essential for maintaining the health and economic prosperity of a community, with significant investments required to install and maintain the infrastructure. For long-term network operation, a regular condition assessment program is required to locate and characterize anomalies, so a targeted repair or removal plan can be implemented. Fluid transients are a potential tool for assessing faults, as different anomalies will have different effects on the reflection and transmission of a transient wave. Measuring the evolution of pressure in the pipe after the controlled generation of a transient wave can therefore allow the anomaly to be identified.

Entrapped air is a pipeline anomaly which can cause problems for network operators. Air pockets can form in water supply pipes through a variety of mechanisms: as dissolved air leaving solution in low pressure regions, or as entrained air entering the flow through joints and fittings or vortex action (Lauchlan et al. 2005). Due to the buoyancy of air, it often collects at high points in the system, either obstructing the main flow path (referred to as an "in-line" pocket), or in cavities beneath valves and hydrants ("off-line"). Similar to a solid blockage, in-line air pockets reduce the pipe cross-section at steady state, resulting in increased energy consumption and pumping cost. Pumping accounts for approximately 75% of the energy costs for a distribution network, and in-line air pockets can increases these costs by up to 30% (Pozos et al. 2010). Although the blockages created by in-line pockets can inflate the operating costs of the system if left unchecked, off-line air pockets do not pose the same risk. Being outside the main flow path, off-line pockets do not create a blockage and are therefore less likely to compromise the hydraulic operation of the system. To optimize the efficiency of network maintenance programs, techniques are needed to differentiate between the two cases in transient condition assessment.

Currently, little is known about the interaction of transients with off-line pockets or how this compares to an in-line pocket. Experimental studies into the transient interaction with an air

pocket in the main flow path have investigated the effects of base flow, pocket volume, and pocket profile for a range of scenarios. These include the effect of air trapped at the end of a dead-end pipe subject to a compression wave (Zhou et al. 2011) (Vasconcelos and Leite 2012) (Hou et al. 2014) (Zhou et al. 2018), the effect of air during the pipe emptying process (Coronado-Hernández et al. 2017) (Fuertes-Miquel et al. 2019), and the effect of large air pockets entirely blocking the flow path (Zhou et al. 2013). These studies have primarily focused on predicting the influence of air on peak surge pressures caused by events such as pump shutdown, meaning transients were generated using long valve movement times (in the order of 0.1-1 seconds) relative to the pipe lengths used. The resultant interference from system boundaries meant that specific features of the air pocket reflection and transmission could not be characterized. High frequency signals are also required to identify the frequency-dependent behaviour specific to air pockets. The area of focus for this study is in-line air pockets located in the middle of the pipe which do not obstruct the flow entirely. The most comparable experimental study is that of Pozos-Estrada (2017), which investigated the transient interaction with large in-line air pockets followed by a hydraulic jump using a rapid solenoid movement, with the air found to reduce the transient amplitude and increase the transient period. Wan et al. (2017) describes an experimental study to better understand the effect of in-line air pockets on flow dynamics and head losses at steady state. Previous work by Alexander et al. (2020) for the in-line pocket scenario showed that the amplitude of the reflected wave could be accurately predicted using impedance theory, with larger pocket volumes resulting in increased reflectivity. The presence of in-line air also results in frequency dependent attenuation, with frequencies above the resonant frequency of the air being suppressed in the transmitted pulse.

Previous transient-based studies regarding off-line collections of air have been most commonly focused on predicting air chamber dynamics. Air chambers utilise the cushioning properties of air for surge protection. Given this application, the focus has been on predicting peak surge pressures, and few experimental studies have focused on the case of smaller air pocket volumes in the order of 1-10 ml. The scope of this study is small air pocket volumes which may feasibly form in unwanted locations and disrupt system operations. Previous field and laboratory tests using

small air pocket volumes have generated transients using pump shutdown or manual valve closure, and studied the influence of air volume and base flow on the maximum and minimum system pressure, cavity pressure, and cavity water level (Di Santo et al. 2002) (Besharat et al. 2016) (Kim et al. 2014). Similar to previous work regarding in-line pockets, the transient generation times are long relative to the pipe length. The low frequency content of the input waves and associated boundary interference means that the specific reflection and transmission characteristics of each pocket configuration could not be observed in detail. Bhattarai et al. (2019) noted that optimization of the air chamber design process has largely focused on numerical analyses. As a result, limited experimental investigations have involved high-frequency transient testing of small off-line pockets using valve movement times in the order of 1-10 ms. Kim (2008b) and Bergant et al. (2018) carried out high-frequency transient testing for the case where the off-line cavity is entirely filled with air and there is no separating water column between the main pipe and the air-water interface. The off-line pocket was found to reduce the local wave speed and created out-of-phase reflections. For this scenario, a simple accumulator model (Wylie et al. 1993) was able to accurately predict the response. However, for pockets which do not fill their cavity, the properties of the connecting fluid section may be important (Kim 2010). Subsequent high-frequency tests by Ferreira et al. (2018) using a small acrylic off-line cavity found that the off-line air introduces additional damping and can amplify transient pressures compared to the no-air case.

The previous studies on air pocket dynamics have only focused on one type of pocket, but no studies have directly compared the behaviour of in-line and off-line pockets within the same experimental system. Such comparisons will identify clear distinguishing features for their identification and provide pipeline operators confidence in implementing invasive bleeding procedures in the case of an in-line air blockage. The purpose of this study is to carry out experimental investigations into the reflection and transmission of a high frequency transient through a pipe with zero base flow with an air pocket part way along its length for a range of air volumes and initial hydrostatic pressures. Two different air pocket configurations were tested: in-line, where the air pocket is located in the main flow path, and off-line, where the pocket is located in a cavity outside the

main pipe. This study focuses on off-line pockets which partially fill the cavity and do not create any flow blockage. The tests for both configurations were carried out on the same experimental system, and the transients were generated using computer-controlled rapid valve movements. This study is part of a series of articles within a broader context on air pocket dynamics, and follows earlier experimental and numerical investigations of the in-line pocket configuration by Alexander et al. (2019) and Alexander et al. (2020). The results are used to identify the effects of pocket configuration on transient behaviour in the time and frequency domains. Any differences in the wave behaviour can lead to techniques to identify whether the air pocket is in- or off-line with the flow and hence determine if it is at risk of causing a restriction of the main flow.

EXPERIMENTAL PROCEDURE

The experimental apparatus shown in Fig. 1 was constructed in the University of Canterbury Fluids Laboratory. The 41.6 m steel pipe has an internal diameter of 22.25 mm, and is set at a constant angle of 3.5°, resulting in a height difference of 2.51 m between the two ends of the pipe. Figure 2 shows the test sections used for the in-line and off-line configurations. For the off-line scenario, a steel cavity 177 mm long (l_{cavity}) with an internal diameter of 8.5 mm (d_{cavity}) was screwed to the top of a steel crest section in the middle of the pipe. At the base of the cavity was a short neck section of length 24.9 mm (l_{neck}) and diameter 6.3 mm (d_{neck}). Air was inserted at the top of the cavity via a bleed valve. For the in-line case, air was inserted directly into the main pipe at the top of the crest section. The air was inserted at room temperature using a measuring syringe, which enabled the volume of air to be measured at atmospheric pressure. Once the test was complete, the air was removed using the syringe and its volume measured again to check that the air had not moved outside the cavity. At the downstream end of the pipe, 27.10 m from the air pocket, was a reservoir to pressurize the system. At the upstream end of the pipe, 14.50 m from the air pocket, was a Baccara GEM-SOL Direct Operated side discharge solenoid valve (2.4 mm orifice, 1/4-inch port) which was programmed to open and close over a period of 6 ms to generate the transient pulse. The pressure disturbances were measured at four locations using PCB Piezotronics Model 102A07 dynamic pressure transducers with a sampling frequency of 10,000 Hz. The transducers have a

345 kPa measuring range, a natural frequency of over 250 kHz, and an uncertainty of 3.45 kPa. PT1 was located at the upstream end next to the solenoid valve. PT2 was located 6.21 m upstream of the air pocket section, while PT3 was located 6.30 m downstream of the air pocket section. PT4 was located at the centre of the crest. The pressure response was recorded by the transducers for five seconds following the generation of the transient, enough time for the system to return to steady-state.

To prevent air being moved to another location by the flow, the tests were carried out with no base flow. The theory governing the air pocket dynamics (Eqns. 3-7, presented in the following section) highlights that the transient response due to an air pocket is governed by the pressure of the air pocket and its volume. The presence of flow does not affect these parameters, so it is expected that the findings may also be applied to scenarios where there is flow in the system. Flow may affect the geometry of the air pocket, but for small pocket volumes such as those used here, these changes will be in the order of 0.01 m, beyond the bandwidth of the input signal. Nine off-line air pocket volumes were tested, ranging from 1.25 ml to 29.4 ml at atmospheric pressure (V = {1.25; 5.0; 8.9; 12.8; 17.1; 21.0; 23.8; 25.7; 29.4} ml). Only air volumes which are fully contained by the off-line cavity are considered in this investigation, as the largest pocket volumes tested have shown that once the off-line pocket volume exceeds the size of the cavity its behaviour tends to that of a similarly sized in-line pocket. Eleven in-line pocket volumes were tested in this range (V = {2.9; 3.5; 7.1; 7.8; 9.9; 11.3; 15.5; 16; 16.5; 21.6; 26.5} ml). The sensitivity of the syringe to hand operation meant identical volumes were not used for each pocket configuration. Tests were run for each air pocket volume at initial hydrostatic pressures ranging between 0.5 bar and 3.0 bar in 0.5 bar increments. Tests were also carried out with no air injected into the system for each configuration to isolate the effect of the off-line attachment. According to Henry's Law (Sander 2015), the increase in pressure will result in some dissolution of the air in the crest section. However, this dissolution is expected to be in the order of 0.01 ml, and is minor compared to the total volume of air inserted. The full volume of air inserted at the beginning of the test was retrieved from the crest section at the end of the test, confirming that no air had dissolved or moved elsewhere in the pipe. To control

experimental error, testing was repeated ten times for each set of experimental conditions. The intervening period between tests was approximately one minute, to ensure the transient disturbances had damped entirely before starting the next test. A standard error was calculated for each time step in each experimental scenario. Over the time period of interest, including the incident pulse and first reflected and transmitted pulses measured at the transducers, the average standard error was less than 0.05% of the pressure reading.

GOVERNING EQUATIONS FOR NUMERICAL SIMULATIONS

Numerical modelling using the Method of Characteristics (MOC) will be used to explain key observations in the time domain. The governing mass and momentum equations for 1D unsteady pipe flow are (Wylie et al. 1993)

$$\frac{\partial U}{\partial t} + g\frac{\partial H}{\partial x} + g h_f = 0 \,, \tag{1}$$

$$\frac{\partial H}{\partial t} + \frac{a^2}{g}\frac{\partial U}{\partial x} = 0 \,, \tag{2}$$

where H is the piezometric head, U the fluid mean velocity, a the pipeline wave speed, x the distance along the pipe, t the time, g acceleration due to gravity, and h_f the friction loss per unit length. These can be used to form positive and negative characteristic equations to solve for velocity and pressure along the pipe at each time step. The approach used is outlined in Alexander et al. (2019), and both steady and unsteady friction are included in the modelling using the weighting function method defined by Zielke (1968).

The simple accumulator model is used to incorporate air pockets into the MOC grid. It is assumed the air pocket behaves according to a polytropic relationship

$$H_A V^n = C_A \,, \tag{3}$$

where H_A is the absolute head at the pocket, V the pocket volume, n the polytropic exponent, and

C_A the polytropic constant which can be calculated using the initial conditions. Wylie and Streeter's model for a simple accumulator is commonly used for in-line pockets and simple off-line pockets, and it neglects inertia and friction in any connecting sections (Wylie et al. 1993). The governing equations are outlined in Alexander et al. (2019). However, for off-line pockets separated from the main pipe by a short water column, friction and inertia in the water column may also be considered (Wylie et al. 1993). This will be referred to as the lumped inertia model. The process is outlined in detail by Karney and McInnis (1992) and Kim (2008a). Based on a discrete linearized momentum equation applied to the connector, at a given time index j the head at the pocket interface is linked to the head at the junction with the main pipe according to the following:

$$H_j^J - H_j^S = C_{c1} + C_{c2} Q_j^{ext} \tag{4}$$

$$C_{c1} = H_{j-1}^S - H_{j-1}^J - \frac{8 l_c}{g \pi D_c^2 \Delta t} Q_{j-1}^{ext} \tag{5}$$

$$C_{c2} = \frac{8 l_c}{g \pi D_c^2 \Delta t} + \frac{16 f_c l_c}{g \pi^2 D_c^5} |Q_{j-1}^{ext}| \tag{6}$$

where H^J is the head at the junction, H^S the head at the water surface, Q^{ext} the flow into the cavity, l_c and D_c the length and diameter of the connection between the main pipe and the air, Δt the time step, and f_c the friction factor of the flow in the connection. The subscript $j-1$ corresponds to the quantities calculated in the previous time step. The friction factor is calculated using the flow velocity in the connection at the end of the previous time step. The inertia and friction contribution in both the cavity and neck section were included in order to obtain the most accurate result. Merging Eqn. 4 with Eqn. 3 and the characteristic equations for flow within the pipe, a relationship can be obtained which contains Q_j^{ext} as the only unknown:

$$\begin{aligned} \left(C_c - B_c Q_j^{ext} + \bar{H} - \left(z_{j-1} + \frac{0.5 \Delta t}{A} (Q_j^{ext} + Q_{j-1}^{ext}) \right) - C_{c1} - C_{c2} Q_j^{ext} \right) * \\ \left(V_{j-1} - 0.5 \Delta t (Q_j^{ext} + Q_{j-1}^{ext}) \right)^n = C_A \end{aligned} \tag{7}$$

In the above equation, $\bar{H}$ is the atmospheric pressure, A is the cross-sectional area of the cavity, and Δt is the time step of the MOC. The term C_c is the MOC constant for the junction calculated using the positive and negative characteristic coefficients (Karney and McInnis 1992).

RESULTS

Time Domain Observations

The experimental investigations involved the collection of pressure measurements both upstream and downstream of the off-line and in-line air pockets, capturing both the reflected and transmitted waves. Note that the pressure responses obtained for the no-air case were comparable for the system configurations with and without the off-line attachment. A minor reflection from the crest section of less than 5% of the incident pulse amplitude was observed for both the in-line and off-line configurations. This indicates that, in this experimental scenario, the cavity alone does not create a significant transient reflection, meaning the observed responses for the air pocket cases may be assumed to be relate predominantly to the presence of the air. In the experiments, the air pocket volumes were measured outside the pipe at atmospheric pressure before and after each test using a measuring syringe. This volume was converted to a pressurised volume inside the pipe (V_p) using the reversible polytropic relation (Eqn. 3). A polytropic exponent of 1.2 was used, as this mid-range value has been commonly used in previous research on air-water interactions (Wylie et al. 1993) (Martin 1976) (Izquierdo et al. 1999) (Carlos et al. 2011). Figure 3 presents measured pressure traces for a range of in-line and off-line air pocket volumes to show the effect of air pocket volume on the response. Figure 4 presents measured pressure traces for a set of in-line and off-line pocket volumes with similar in-pipe volumes (within 5% of the average V_p quoted in the figure caption) at a range of initial hydrostatic pressures, to show the effect of initial pressure on the response. The pressure traces presented have been normalized by the initial hydrostatic pressure such that $H^* = \frac{H}{H_0}$, where H is the measured pressure disturbance at any time and H_0 is the steady state initial hydrostatic pressure. The elapsed time t is normalized by the pipeline period $T = \frac{4L}{a}$, calculated using the pipe length, L, and the experimental wave speed (1348.5 m/s). The experimental wave speed was estimated by cross-correlating the transient traces measured at

PT1 and PT2 for the no-air case. The time lag at which the cross-correlation of the two signals was maximized represents the pulse travel time between the two sensors. The solenoid movement generating the transient commences at $t* \approx 0.085$.

The first waves reflected and transmitted by the air pockets have been boxed and labelled in Figs. 3 and 4. Several key differences were observed between the two configurations, particularly with regard to the sharpness of the reflected and transmitted pulses. This indicates that the in-line and off-line have different frequency dependent effects. The pulses from both pockets are followed by extended low pressure tails. This may also be observed for a solid blockage (Meniconi et al. 2016). The sharpness of the transmitted pulse for the off-line configuration suggests that majority of the incident pulse's high frequency content is transmitted. The converse is true for the in-line configuration. These differing effects mean that as the transient progresses the shape of the pressure trace for the off-line pocket case varies significantly from that measured for the in-line pocket case. The frequency-dependent response is explored in further detail in the following section.

Numerical modelling can be used to explain the difference in transient shape observed for the in-line and off-line air pocket cases. The simple accumulator model has previously been used to model the in-line pocket scenario, and though it was found to result in timing and amplitude errors it was able to capture the general shape of the transient response (Alexander et al. 2019). It has also been used in previous research to successfully model the off-line case where the air entirely fills the cavity and there is no connecting water column (Kim 2008b). The outputs of the simple accumulator and lumped inertia models are compared to the experimental observations upstream and downstream of the pocket section for the off-line air pocket in Figs. 5 and 6, which correspond to air pockets occupying 16% and 75% of the cavity respectively. The lumped inertia model predicted the response for the off-line case with much greater accuracy than the simple accumulator model across the range of volumes tested. Repetition of the lumped inertia modelling with inertia included, but without friction in the cavity and neck, resulted in a maximum difference of 3.9% in the modelled output for the first reflected and transmitted peaks. This indicates that inertia in the cavity and connector was the primary cause of the differences observed in the response due to air

pocket configuration. In the field off-line pockets may not entirely fill their confining cavity, such as those connecting hydrants to the main pipe, meaning the inertia effects identified represent a distinction between the two configurations in real-world applications. Key features captured by the lumped inertia model include the smoothing of the low pressure tail following the reflected pulse, and the high frequency pressure fluctuations created during transmission.

The damping of the transient signal is expected to follow an exponential function (Wang et al. 2002). This can be fitted by obtaining the average transient amplitude in the time domain or the harmonic amplitude in frequency domain for each period of the transient trace. The exponent of the exponential function represents the damping rate. The average amplitude per period in the time domain for the no-air case and example in-line and off-line pockets is shown in Fig. 7. The three scenarios follow exponential damping trends. For the no-air case, the damping rate ranged between 0.13 and 0.19 for the experimental settings tested. Figure 7 shows that the presence of air significantly increases the damping rate to an average rate of 0.40 for the in-line air configuration, which was consistent across the range of pocket volumes tested. Greater variation with pocket volume was evident for the off-line case, where the damping rate increased with pocket volume from 0.29 to 0.55 across the range tested. The 95% confidence intervals included on Fig. 7 for the exponential fit show that damping may be subject to greater variability for the air pocket case. This may be attributable to the frequency dependent effects of air.

Frequency Domain Observations

A discrete Fourier transform (DFT) can be used to quantify the frequency distribution of the incident, reflected, and transmitted pulses for each air pocket configuration. The DFT was carried out on the entire pulse, meaning both the main peak and extended tails of the reflected and transmitted waves were included in the analysis. Figure 8 compares the DFT amplitudes of the frequencies contained in the incident and resultant pulses for in-line and off-line air volumes. The DFT amplitude is normalized by the initial hydrostatic pressure ($h^* = \frac{h}{H_0}$), while the frequency is normalized by the pipeline fundamental frequency ($\omega^* = \frac{4L}{a}\omega$).

The general trends observed in Fig. 8 are consistent across the range of pocket volumes

tested. The incident pulse for both configurations contains frequencies ranging between $\omega^* = 0$ and $\omega^* = 70$. It has been observed in previous work that the in-line air pocket response is frequency dependent, with high frequency content ($\omega^* > 20$) being primarily reflected by the pocket (Alexander et al. 2020). For the in-line pocket, the cut-off frequency, where the transmitted DFT amplitude is first less than 5% of the incident DFT amplitude, was identified as a diagnostic tool (marked in Fig. 8(a)). The cut-off frequency was found to increase with decreasing pocket volume. For the off-line pocket configuration, the DFT showed that the reflection contained a frequency band ranging between $\omega^* = 0$ and $\omega^* \approx 35$. The reflected DFT amplitude reached a peak, corresponding to a local minimum in the transmitted frequency distribution, at $\omega^* \approx 3$, though this value decreased with increasing pocket volume. The high frequency content outside this range was primarily transmitted.

The frequency dependent effects observed are unique to air pockets due to their compressibility; other common faults such as leaks and solid blockages do not impose such changes on the shape of the incident pulse (Brunone 1999) (Meniconi et al. 2011). A physical understanding of the frequency dependent effects of off-line pockets could be used to inform condition assessment techniques. The reflectivity of a pipeline anomaly such as the off-line air pocket is determined by its impedance relative to that of the main pipe. Previous research by Wylie (1965) states that impedance may be maximized at the resonant frequency of a system. In the medical field, theory has been developed to estimate the resonant frequency of air bubble within a blood vessel (Jang et al. 2009). The same principles may be able to predict the effects of off-line pockets in water supply infrastructure. The resonant frequency, ω, of an air pocket confined to a tube can be obtained from

$$\left(\frac{\omega}{\omega_0}\right)^2 = \frac{r_{cavity}^2}{4R_0}\left(\frac{1}{L_1 - \frac{l_p}{2} + \Delta L} + \frac{1}{L_2 - \frac{l_p}{2} + \Delta L}\right), \tag{8}$$

where r_{cavity} is the radius of the confining cavity, R_0 is the radius of the sphere which would be formed by the same pocket volume in an infinite fluid domain, L_1 and L_2 are the length of pipe from the centre of the pocket to the end of the cavity in each direction, l_p is the length of the pocket, and ΔL is an end correction factor given as $0.62 r_{cavity}$, which accounts for the inertia of liquid outside

the cavity (Jang et al. 2009). This end correction factor was determined theoretically by Levine and Schwinger (1948). The resonant frequency of the same pocket in an infinite fluid domain, ω_0, is calculated by

$$\omega_0 = \frac{1}{2\pi R_0}\sqrt{\frac{3nP_0}{\rho}}\,, \tag{9}$$

where n is the polytropic exponent, P_0 is the ambient pressure, and ρ is the fluid density (Minnaert 1933). The resonant frequency of the off-line air pocket therefore varies with its volume, pressure, and the dimensions of the cavity it is confined to. A limitation of the application of Eqns. 8 and 9 in this situation is that the transient nature of the problem means that the pressure and volume of the pocket are constantly changing. However, modelling using the lumped inertia approach introduced previously suggested that the maximum variation in the resonant frequency due to transient effects was less than 2%, meaning that for these experiments the resonant frequency at steady state can be considered representative for the transient duration. Figure 9 shows the theoretical resonant frequencies for the range of experimental scenarios compared to the local minimum frequency of the transmitted pulse DFT, which will be referred to as the primary suppressed frequency (marked in Fig. 8(b)). The suppressed frequency was used because the off-line pocket resulted in some irregularities in the reflected pulse DFT at low frequencies ($\omega^* < 4$). In general, the theoretical resonant frequency agreed well with the frequency at which the transmitted DFT reached a local minimum, supporting the hypothesis that the reflectivity of the pocket was maximized due to resonance. The average error between the theoretical and observed resonant frequencies was approximately 11%. Figure 10 shows that the experimental primary suppressed frequency also increased with initial hydrostatic pressure for a given in-pipe volume of air. This is in agreement with Eqn. 9. Similar to the time domain observations, the response of the pocket in the frequency domain was dependent on both the pocket volume and the cavity characteristics.

CONCLUSIONS AND RECOMMENDATIONS

The effects of air pocket configuration on high frequency transient reflection and transmission have not previously been investigated experimentally. This study compares experimental observa-

tions for similar air pocket volumes in the main flow path (in-line), and in a cavity adjacent to the flow (off-line). The results can be used in transient detection programs to differentiate in-line pockets which are blocking the main flow from off-line pockets which do not obstruct flow, improving the efficiency of network maintenance operations.

Variations observed in the time domain between the two configurations were due to differing frequency-dependent effects. Numerical modelling showed that the variations were primarily due to inertia in the water column connecting the off-line pocket to the main pipe, meaning that both the pocket volume and the cavity characteristics influenced the transient response. Further analysis in the frequency domain was used to quantify the frequency dependent effects of pocket configuration. It was found that the reflectivity of the off-line pocket is maximized at the resonant frequency of the air pocket, with good agreement observed between theoretical and experimental results. In-line air may be characterized using a cut-off frequency, above which signal content is reflected. The observations in the frequency domain have identified a useful approach for differentiating between the two pocket configurations during transient detection. The defining DFT features (the cut-off frequency and the primary suppressed frequency) are simple to distinguish and may also be used to characterize the pocket size. This will enable maintenance resources to focus on potentially more significant in-line air blockages. This further emphasizes the need for high frequency wave testing, as the input signal must contain the frequency range needed to identify these features. The transient damping rate may also be used to diagnose air as a preliminary step.

This study was limited by the breadth of experimental conditions considered, with the potential for other scenarios to be investigated in the future. The tests were carried out without any base flow, which may affect the geometry of the in-line pocket, which is more susceptible to movement and shearing due to its location in the main flow path. This study also only considered pockets which were entirely in-line or off-line. However, in the field pockets may form in off-line cavities and become large enough to intrude into the main flow path. Further testing would provide greater understanding of whether it is possible to characterize this case.

DATA AVAILABILITY STATEMENT

All data, models, or code that support the findings of this study are available from the corresponding author upon reasonable request.

ACKNOWLEDGMENTS

We would like to thank Hong Kong Research Grants Council for the theme based research scheme (TRS) Grant No. T21-602/15R for supporting this research.

NOTATION

The following symbols are used in this paper:

A = pipe cross-sectional area

a = pipeline wave speed

C_A = polytropic constant

D = pipe diameter

d_{cavity} = off-line cavity diameter

d_{neck} = off-line neck diameter

$d_{connector}$ = off-line cavity connector diameter

H = pressure head

h = DFT amplitude

h_f = total friction loss

i = spatial index

j = temporal index

L = pipe length

l_{cavity} = off-line cavity length

l_{neck} = off-line neck diameter

$l_{connector}$ = off-line cavity connector length

n = polytropic exponent

P = pressure

P_0 = ambient pressure

Q = flow

r = pipe radius

r_{cavity} = off-line cavity radius

R_0 = air pocket radius assuming a sphere

t = time

U = velocity

$\forall_p$ = pressurized air pocket volume

$\forall_{cavity}$ = off-line cavity volume

$\forall_{pipe}$ = pipe volume

W = weighting function

x = distance

z = elevation

ν = kinematic viscosity

ρ = density and

ω = frequency.

REFERENCES

Alexander, J., Lee, P. J., Davidson, M., Duan, H.-F., Li, Z., Murch, R., Meniconi, S., and Brunone, B. (2019). "Experimental validation of existing numerical models for the interaction of fluid transients with in-line air pockets." *Journal of Fluids Engineering*, 141(12), 1–9.

Alexander, J., Lee, P. J., Davidson, M., Li, Z., Murch, R., Duan, H.-F., Meniconi, S., and Brunone, B. (2020). "Experimental investigation of the interaction of fluid transients with an in-line air pocket." *Journal of Hydraulic Engineering*, 146(3).

Bergant, A., Tijsseling, A., Kim, Y.-i., Karadžić, U., Zhou, L., Lambert, M. F., and Simpson, A. R. (2018). "Unsteady pressures influenced by trapped air pockets in water-filled pipelines.." *Strojniski Vestnik/Journal of Mechanical Engineering*, 64(9).

Besharat, M., Tarinejad, R., and Ramos, H. M. (2016). "The effect of water hammer on a confined air pocket towards flow energy storage system." *Journal of Water Supply: Research and Technology-Aqua*, 65(2), 116–126.

Bhattarai, K. P., Zhou, J., Palikhe, S., Pandey, K. P., and Suwal, N. (2019). "Numerical modeling and hydraulic optimization of a surge tank using particle swarm optimization." *Water*, 11, 715.

Brunone, B. (1999). "Transient test-based technique for leak detection in outfall pipes." *Journal of Water Resources Planning and Management*, 125(5), 302–306.

Carlos, M., Arregui, F., Cabrera, E., and Palau, C. (2011). "Understanding air release through air valves." *Journal of Hydraulic Engineering*, 137(4), 461–469.

Coronado-Hernández, O. E., Fuertes-Miquel, V. S., Besharat, M., and Ramos, H. M. (2017). "Experimental and numerical analysis of a water emptying pipeline using different air valves." *Water*, 9(2), 98.

Di Santo, A. R., Fratino, U., Iacobellis, V., and Piccinni, A. F. (2002). "Effects of free outflow in rising mains with air chamber." *Journal of Hydraulic Engineering*, 128(11), 992–1001.

Ferreira, J., Ghezzi, E., Ferrante, M., and Covas, D. (2018). "Pressure wave behaviour due to entrapped air in hydraulic transient events." *13th International Conference on Pressure Surges*.

Fuertes-Miquel, V. S., Coronado-Hernández, O. E., Iglesias-Rey, P. L., and Mora-Meliá, D. (2019). "Transient phenomena during the emptying process of a single pipe with water–air interaction." *Journal of Hydraulic Research*, 57(3), 318–326.

Hou, Q., Tijsseling, A. S., Laanearu, J., Annus, I., Koppel, T., Bergant, A., Vučković, S., Anderson, A., and van't Westende, J. M. (2014). "Experimental investigation on rapid filling of a large-scale pipeline." *Journal of Hydraulic Engineering*, 140(11), 04014053.

Izquierdo, J., Fuertes, V., Cabrera, E., Iglesias, P., and Garcia-Serra, J. (1999). "Pipeline start-up with entrapped air." *Journal of Hydraulic Research*, 37(5), 579–590.

Jang, N. W., Gracewski, S. M., Abrahamsen, B., Buttaccio, T., Halm, R., and Dalecki, D. (2009). "Natural frequency of a gas bubble in a tube: Experimental and simulation results." *The Journal of the Acoustical Society of America*, 126(1), EL34–EL40.

Karney, B. W. and McInnis, D. (1992). "Efficient calculation of transient flow in simple pipe networks." *Journal of Hydraulic Engineering*, 118(7), 1014–1030.

Kim, S.-G., Lee, K.-B., and Kim, K.-Y. (2014). "Water hammer in the pump-rising pipeline system with an air chamber." *Journal of Hydrodynamics*, 26(6), 960–964.

Kim, S. H. (2008a). "Impulse response method for pipeline systems equipped with water hammer protection devices." *Journal of Hydraulic Engineering*, 134(7), 961–969.

Kim, S.-H. (2010). "Design of surge tank for water supply systems using the impulse response method with the ga algorithm." *Journal of Mechanical Science and Technology*, 24(2), 629–636.

Kim, Y. I. (2008b). "Advanced numerical and experimental transient modelling of water and gas pipeline flows incorporating distributed and local effects." Ph.D. thesis, University of Adelaide, Adelaide, Australia, University of Adelaide, Adelaide, Australia.

Lauchlan, C., Escarameia, M., May, R., Burrows, R., and Gahan, C. (2005). "Air in pipelines: A literature review." Vol. 649, HR Wallingford. Report SR, Oxford, United Kingdom.

Levine, H. and Schwinger, J. (1948). "On the radiation of sound from an unflanged circular pipe." *Physical review*, 73(4), 383–406.

Martin, C. (1976). "Entrapped air in pipelines." *Proceedings of the 2nd International Conference on Pressure Surges*, Vol. 2, British Hydromechanics Research Association Bedford, UK, September 6-8, 15–27.

Meniconi, S., Brunone, B., and Ferrante, M. (2011). "In-line pipe device checking by short-period analysis of transient tests." *Journal of Hydraulic Engineering*, 137(7), 713–722.

Meniconi, S., Brunone, B., Ferrante, M., and Capponi, C. (2016). "Mechanism of interaction of pressure waves at a discrete partial blockage." *Journal of Fluids and Structures*, 62, 33–45.

Minnaert, M. (1933). "On musical air-bubbles and the sounds of running water." *The London, Edinburgh, and Dublin Philosophical Magazine and Journal of Science*, 16(104), 235–248.

Pozos, O., Gonzalez, C. A., Giesecke, J., Marx, W., and Rodal, E. A. (2010). "Air entrapped in gravity pipeline systems." *Journal of Hydraulic Research*, 48(3), 338–347.

Pozos-Estrada, O. (2017). "Investigation of the combined effect of air pockets and air bubbles on

fluid transients." *Journal of Hydroinformatics*, 376–392.

Sander, R. (2015). "Compilation of Henry's law constants (version 4.0) for water as solvent." *Atmospheric Chemistry & Physics*, 15(8).

Vasconcelos, J. G. and Leite, G. M. (2012). "Pressure surges following sudden air pocket entrapment in storm-water tunnels." *Journal of Hydraulic Engineering*, 138(12), 1081–1089.

Wan, W.-y., Li, C.-y., and Yu, Y.-q. (2017). "Investigation on critical equilibrium of trapped air pocket in water supply pipeline system." *Journal of Zhejiang University-SCIENCE A*, 18(3), 167–178.

Wang, X.-J., Lambert, M. F., Simpson, A. R., Liggett, J. A., and V ı´ tkovskỳ, J. P. (2002). "Leak detection in pipelines using the damping of fluid transients." *Journal of Hydraulic Engineering*, 128(7), 697–711.

Wylie, E. B. (1965). "Resonance in pressurized piping systems." Ph.D. thesis, University of Michigan, Ann Arbor, USA, University of Michigan, Ann Arbor, USA.

Wylie, E. B., Streeter, V. L., and Suo, L. (1993). *Fluid transients in systems*, Vol. 1. Prentice Hall Englewood Cliffs, NJ.

Zhou, L., Liu, D., and Karney, B. (2013). "Investigation of hydraulic transients of two entrapped air pockets in a water pipeline." *Journal of Hydraulic Engineering*, 139(9), 949–959.

Zhou, L., Liu, D., Karney, B., and Zhang, Q. (2011). "Influence of entrapped air pockets on hydraulic transients in water pipelines." *Journal of Hydraulic Engineering*, 137(12), 1686–1692.

Zhou, L., Wang, H., Karney, B., Liu, D., Wang, P., and Guo, S. (2018). "Dynamic behavior of entrapped air pocket in a water filling pipeline." *Journal of Hydraulic Engineering*, 144(8), 04018045.

Zielke, W. (1968). "Frequency-dependent friction in transient pipe flow." *Journal of Basic Engineering*, 90(1), 109–115.

List of Figures

Fig. 1. Diagram of experimental set-up

Fig. 2. Section A-A': Diagram of air pocket configurations (a) in-line, (b) offline. An example pocket profile is filled in gray.

Fig. 3. Experimental pressure disturbances for a range of in-line and off-line air pocket volumes at an initial hydrostatic pressure of 3.0 bar: (a) In-line configuration trace measured at PT2, upstream of the pocket, (b) In-line configuration trace measured at PT3, downstream of the pocket, (c) Off-line configuration trace measured at PT2, and (d) Off-line configuration trace measured at PT3.

Fig. 4. Experimental pressure disturbances for in-line ($V_p \approx 6.6$ ml) and off-line ($V_p \approx 5.2$ ml) air pockets at a range of initial hydrostatic pressures: (a) In-line configuration trace measured at PT2 upstream of the pocket, (b) In-line configuration trace measured at PT3 downstream of the pocket, (c) Off-line configuration trace measured at PT2 , and (d) Off-line configuration trace measured at PT3.

Fig. 5. Experimental and modelled transient pressure traces for an off-line air pocket (V_p = 1.59 ml) at 3.0 bar for (a) Pressure trace measured at PT2, upstream of the pocket, and (b) Pressure trace measured at PT3, downstream of the pocket.

Fig. 6. Experimental and modelled transient pressure traces for an off-line air pocket (V_p = 7.56 ml) at 3.0 bar for (a) Pressure trace measured at PT2, upstream of the pocket, and (b) Pressure trace measured at PT3, downstream of the pocket.

Fig. 7. Average absolute amplitude per period measured at PT1 for the (a) no-air case, (b) in-line pocket (V_p = 5.24 ml) and (c) off-line pocket (V_p = 5.43 ml), alongside exponential fits and 95% confidence intervals for each scenario.

Fig. 8. DFT amplitude of incident, reflected, and transmitted pulses at an initial hydrostatic pressure of 3.0 bar for (a) in-line air pocket (V_p = 5.24 ml), and (b) off-line air pocket (V_p = 5.43 ml).

Fig. 9. Comparison of the primary suppressed frequency observed in the transmitted pulse DFTs with the theoretical resonant frequency of the air pockets. Corresponding experimental and theoretical results are linked by dotted lines.

Fig. 10. Primary suppressed frequency for a range of initial hydrostatic pressures.

Figure 1

Click here to access/download;Figure;Fig1.eps

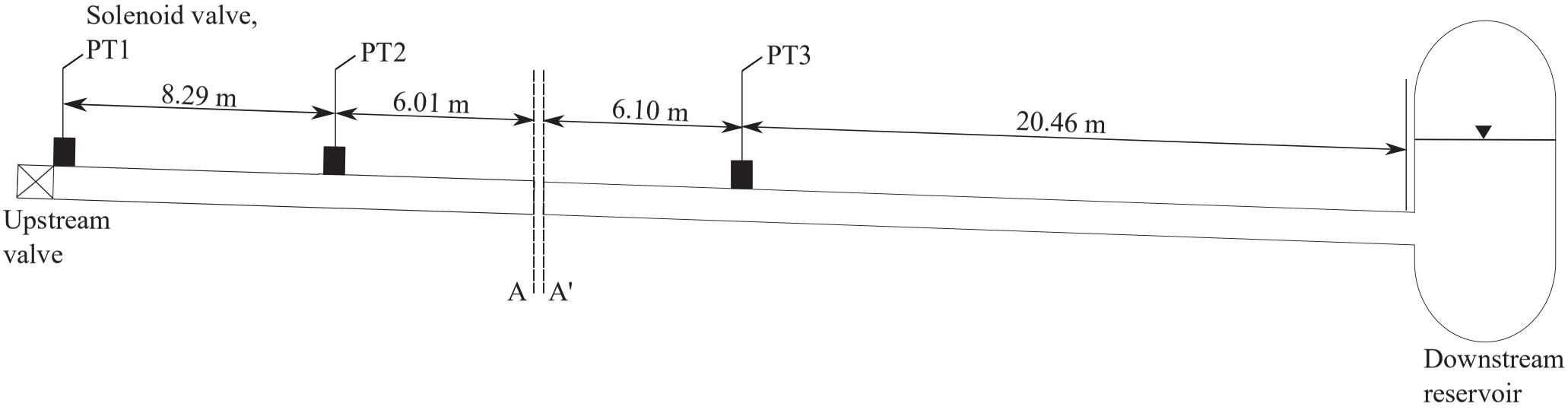

Figure 2

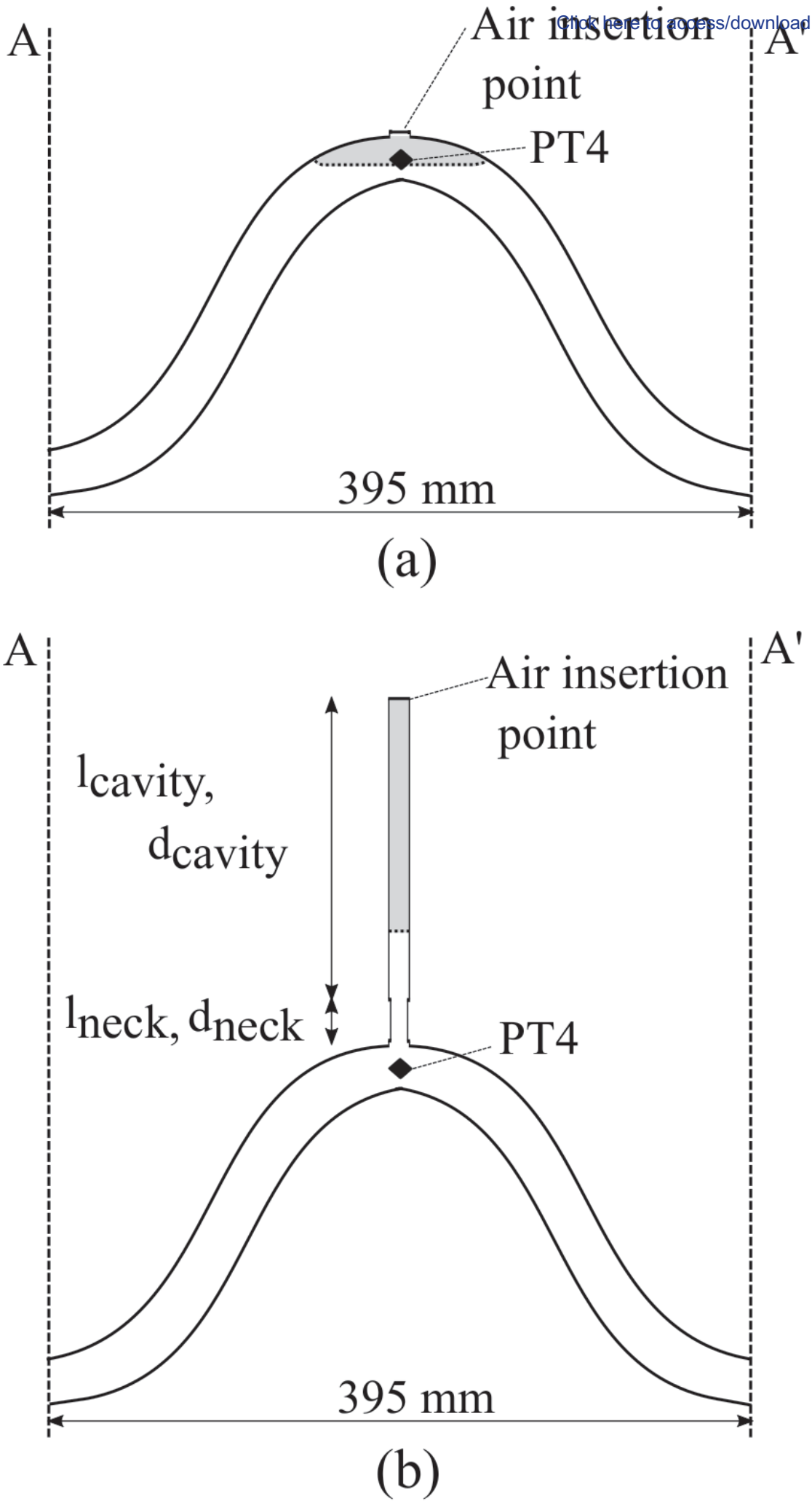

Figure 3

Click here to access/download;Figure;Fig3.eps

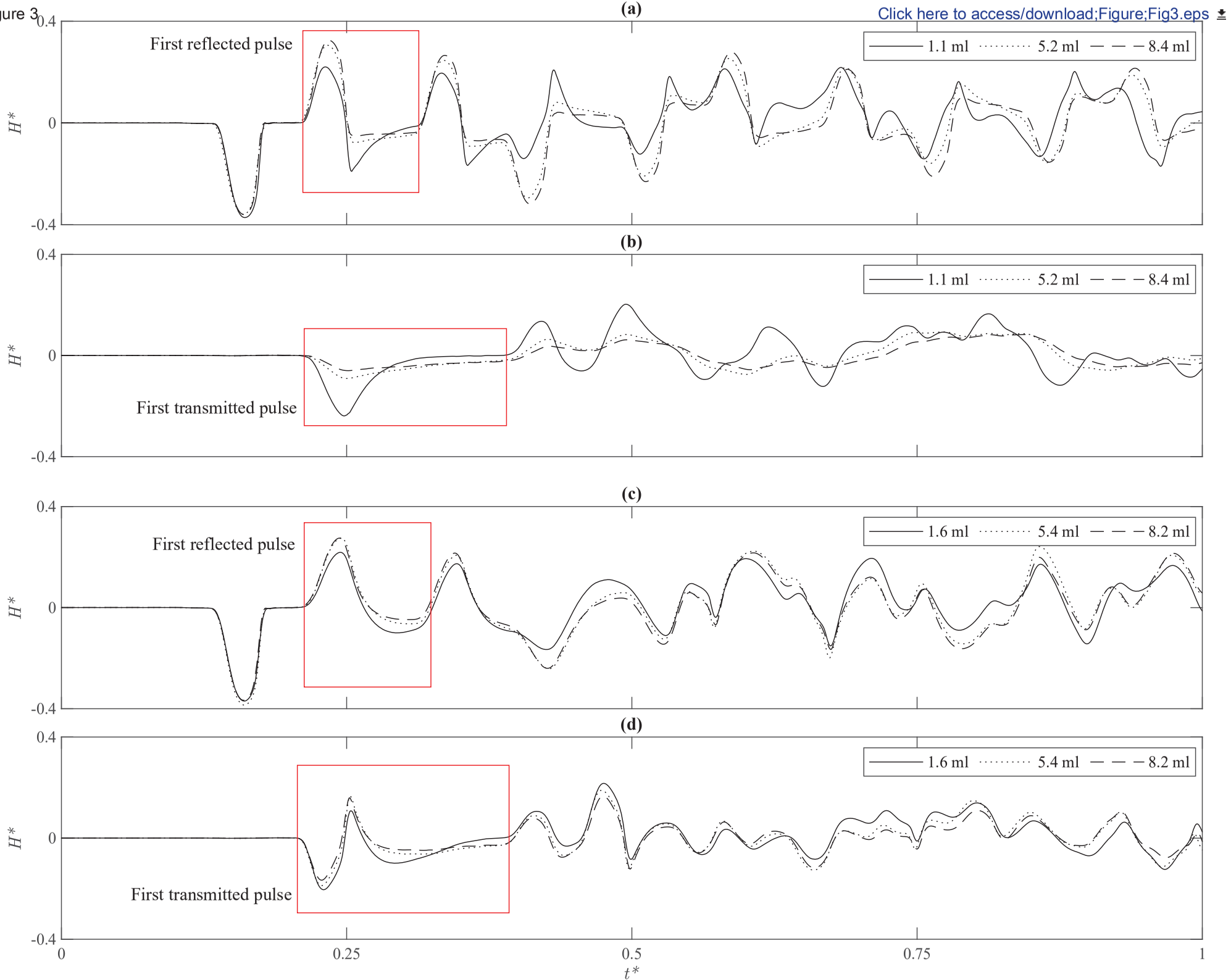

Figure 4

Click here to access/download;Figure;Fig4.eps

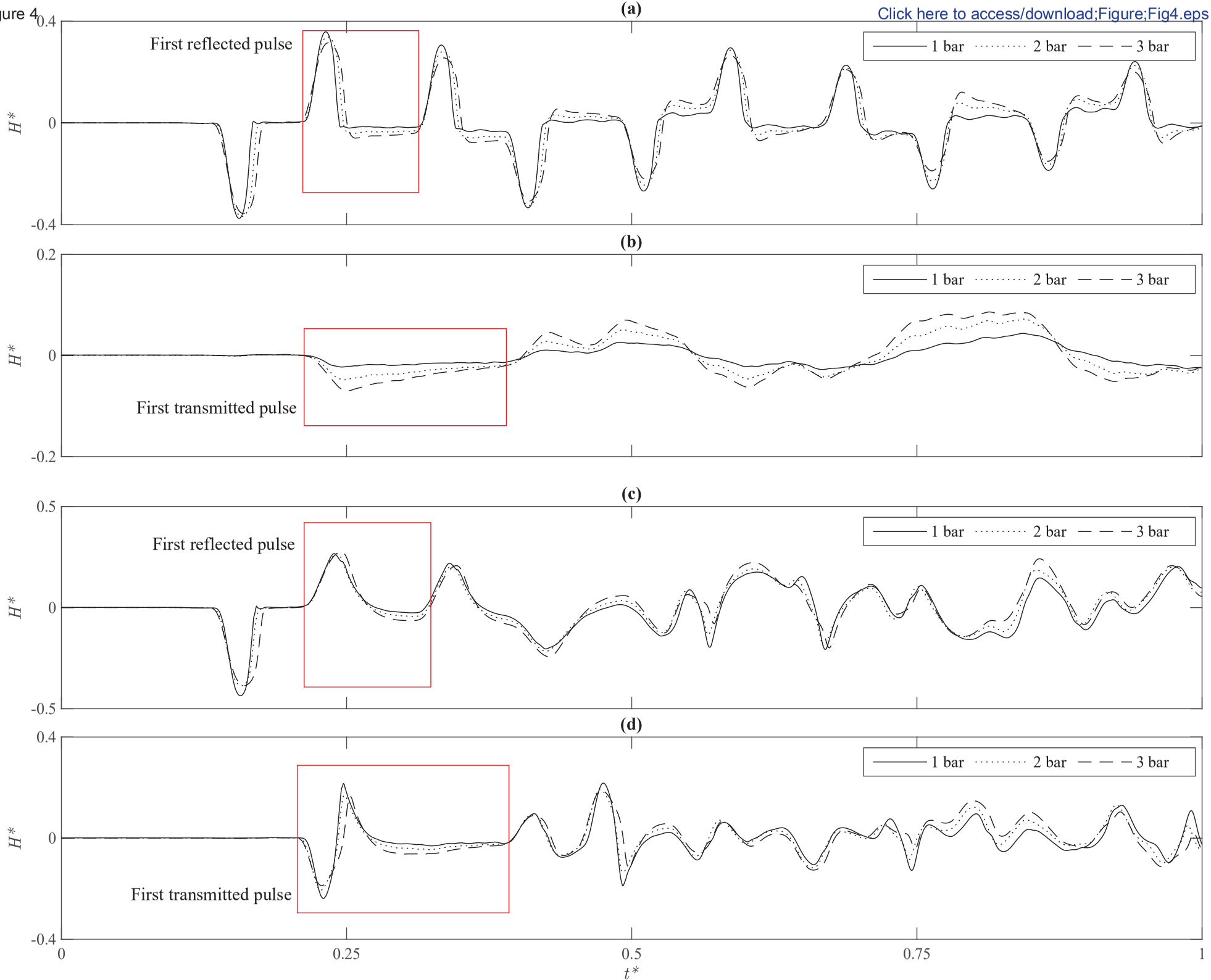

Figure 5

Click here to access/download;Figure;Fig5.eps

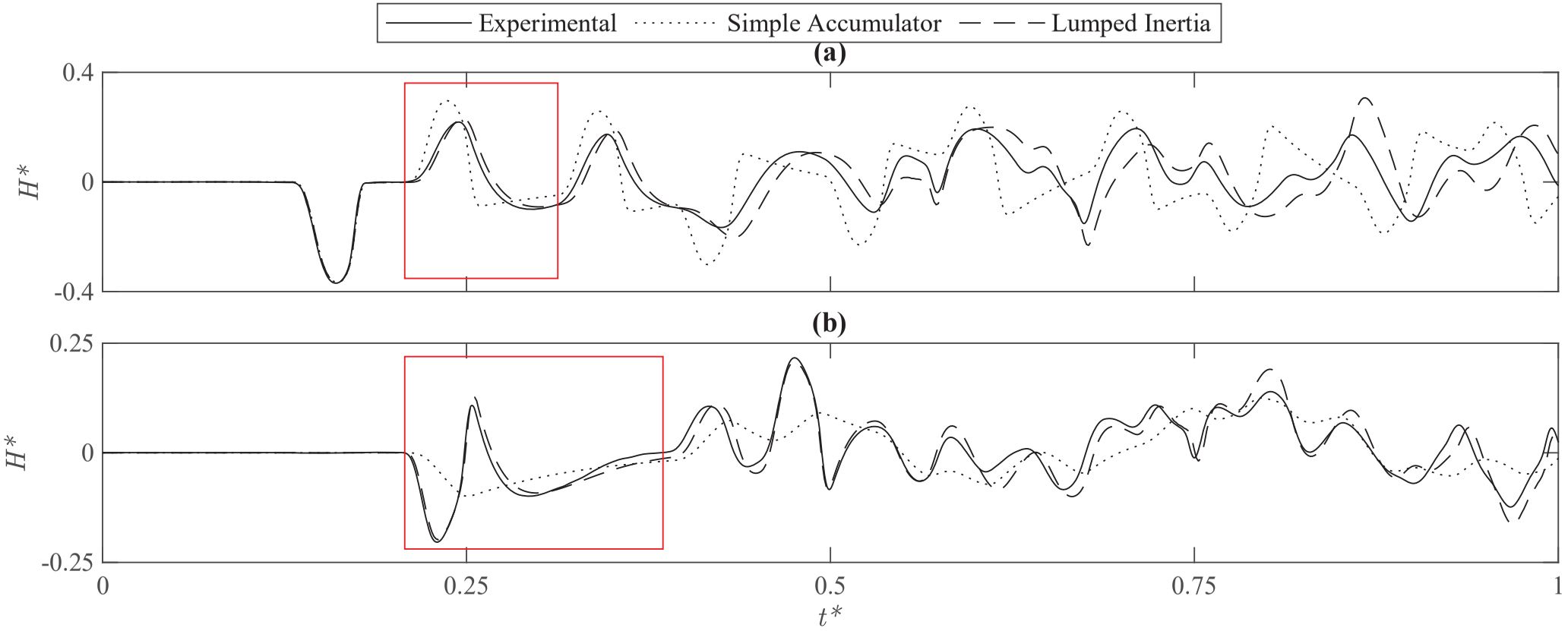

Figure 6

Click here to access/download;Figure;Fig6.eps

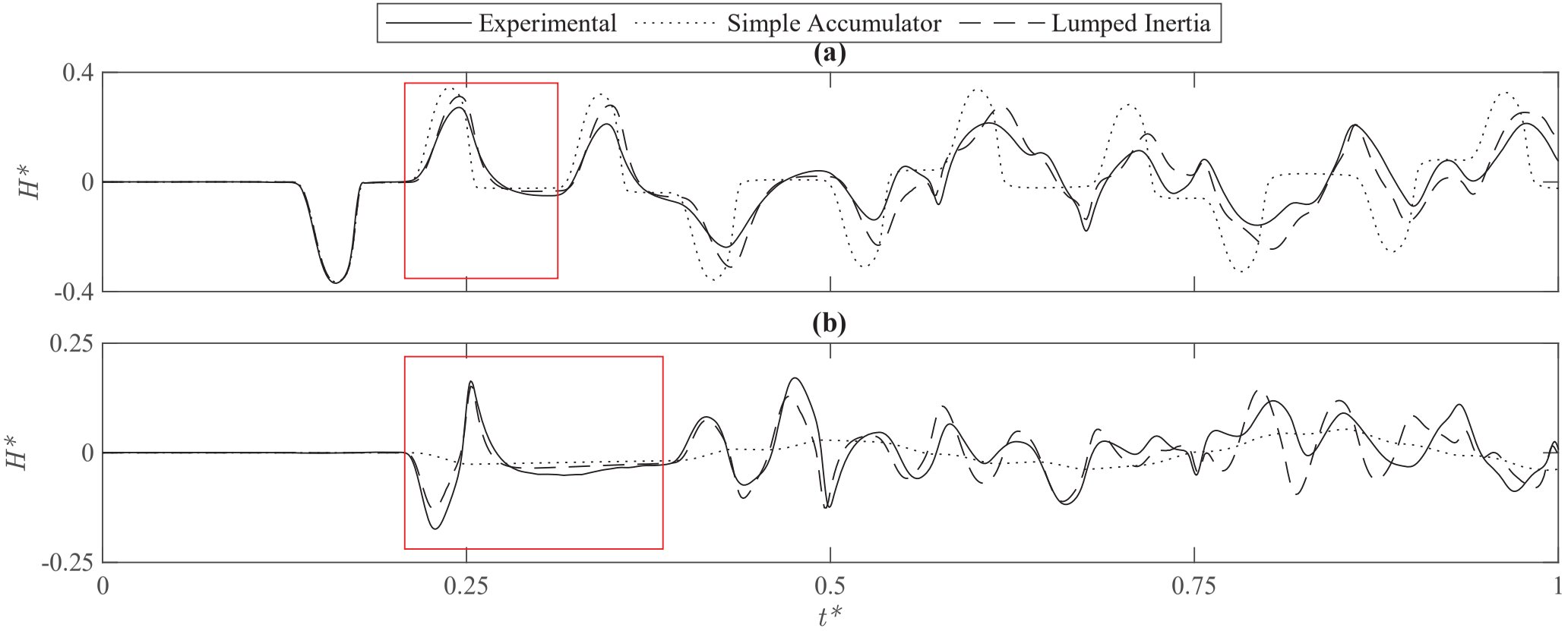

Figure 7

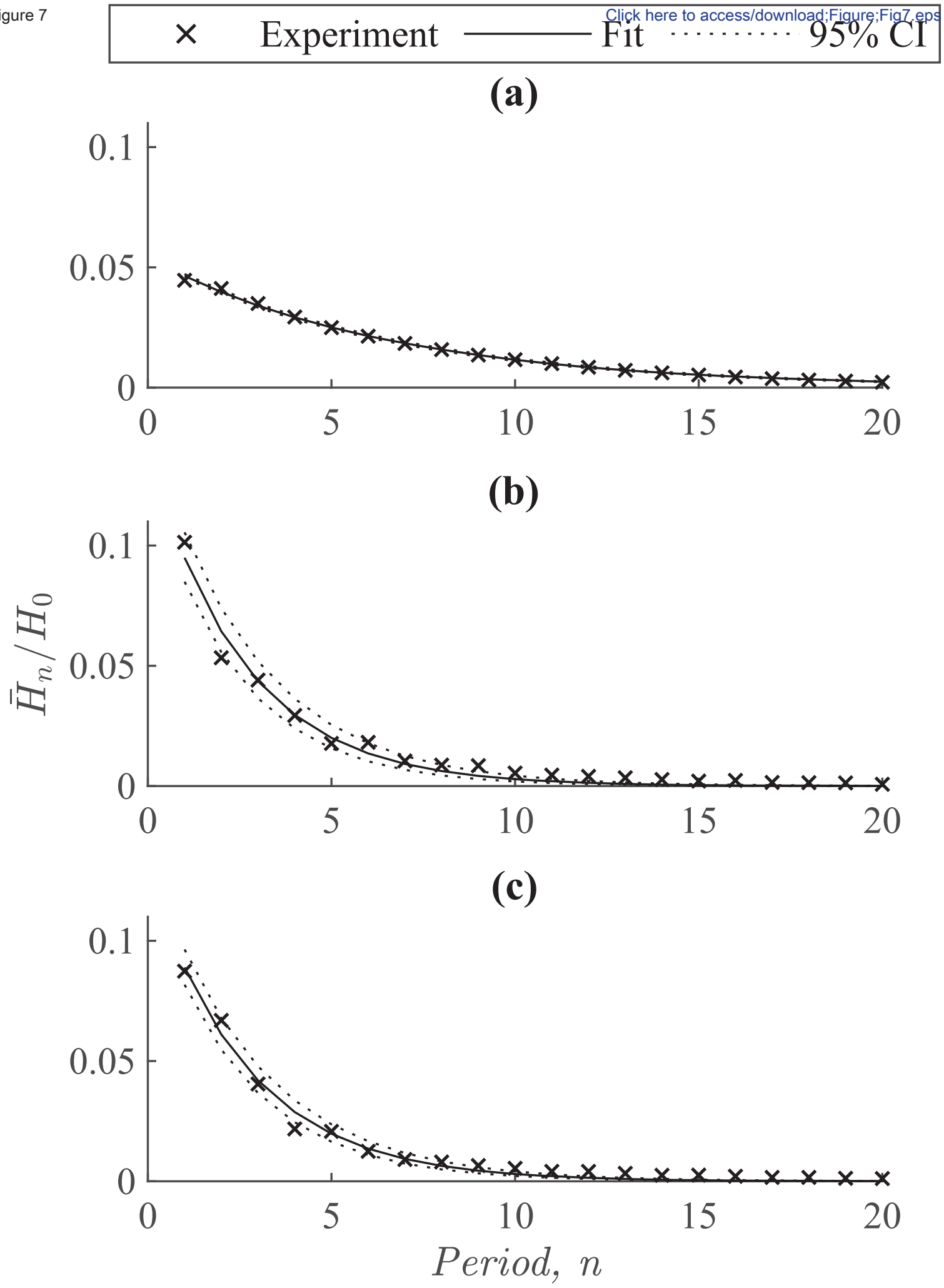

Figure 8

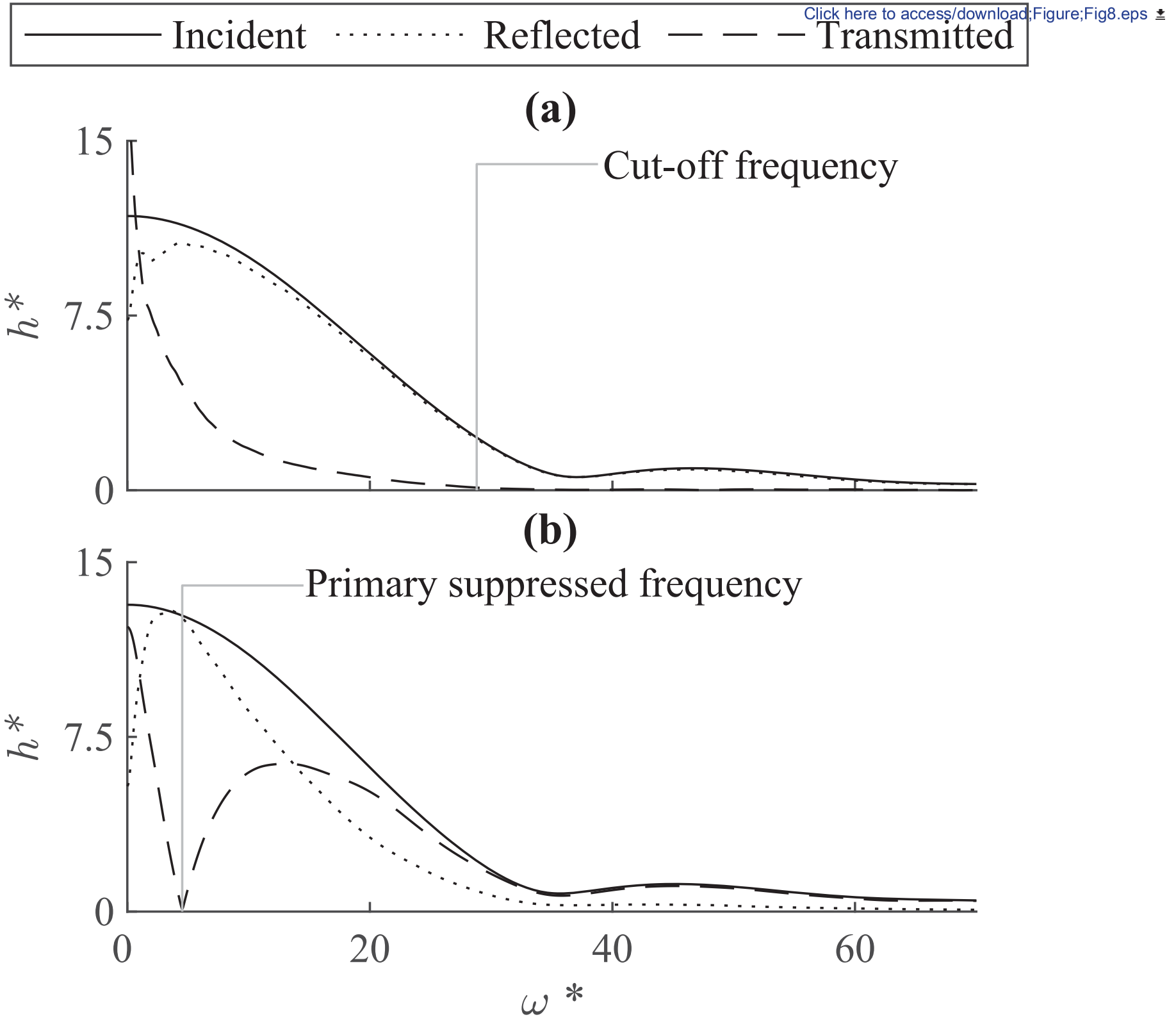

Figure 9

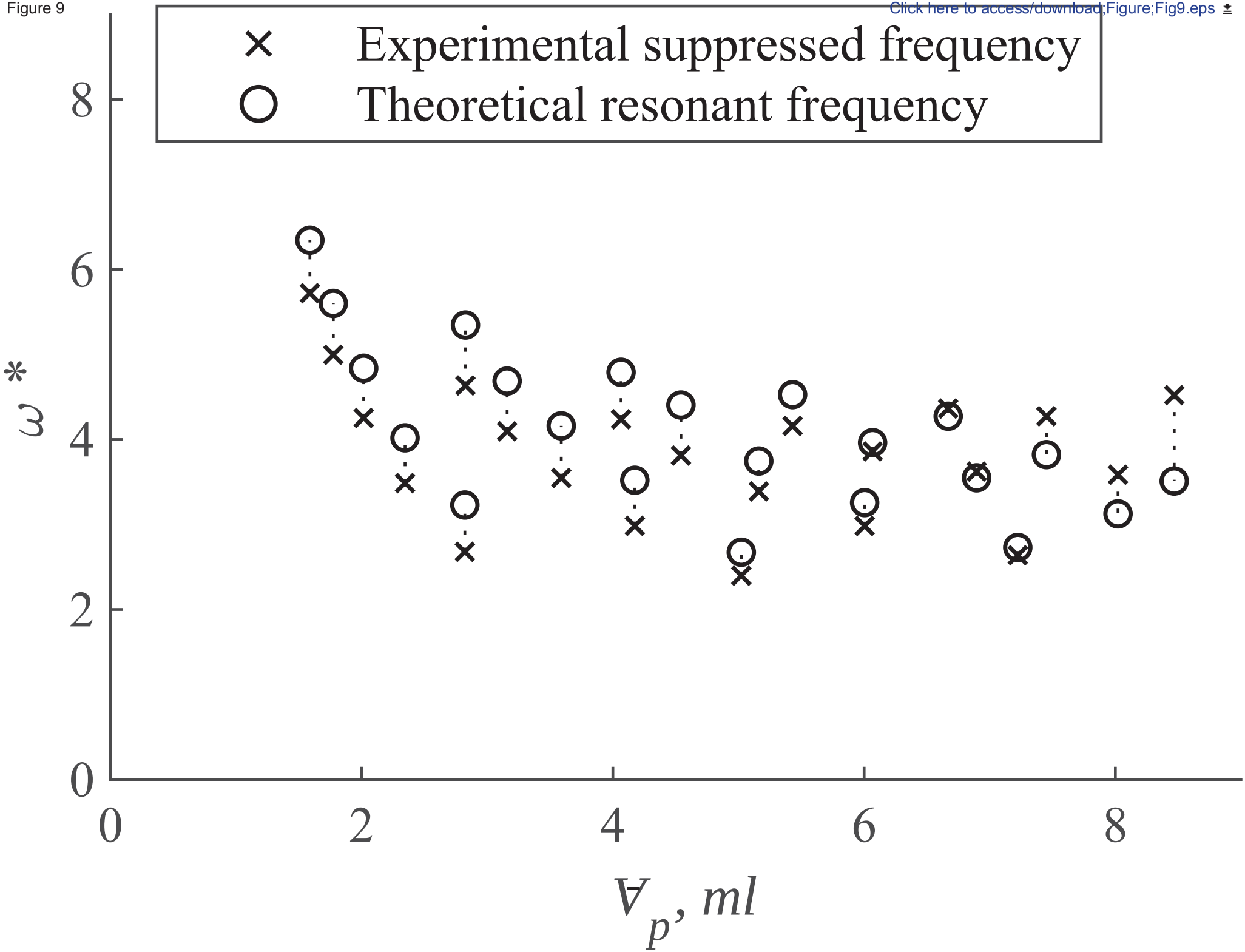

Figure 10